Large-scale circulation over and around the Northern Kerguelen Plateau

Young-Hyang Park[a,*], Fabien Roquet[a], Isabelle Durand[a], Jean-Luc Fuda[b]

[a]*LOCEAN/USM 402, Département Milieux et Peuplements Aquatiques, Muséum National d'Histoire Naturelle, 43 rue Cuvier, 75231 Paris Cedex 05, France*
[b]*Centre Océanologique de Marseille, Campus de Luminy, 13282 Marseille Cedex 09, France*

Abstract

The Kerguelen Plateau is known to constitute a major barrier to the eastward-flowing Antarctic Circumpolar Current. However, there is limited knowledge on the regional circulation due to sparse observations, especially in the Northern Kerguelen Plateau between the Fawn Trough and the Kerguelen Islands. As part of the physical component of the multidisciplinary KEOPS cruise, systematic CTD measurements along three SW-NE oriented sections were made on the latter plateau cutting through the annual phytoplankton bloom across the eastern flank of the plateau into deep water. Major hydrographic features and geostrophic velocities perpendicular to the sections were first documented from these in situ observations. In order to interpret the results within the general circulation context and to trace the upstream pathways of the observed water masses, we established a synthetic picture of the large-scale circulation over and around the entire Northern Kerguelen Plateau, using the combination of new data from KEOPS with historical hydrographic data together with all available information on mid-depth and near-surface velocities derived from autonomous floats, surface drifting buoys, and satellite altimetry. This synthesis shows that the time-mean geostrophic flow over the shallow platform is sluggish (of the order of $3–5\,\mathrm{cm\,s^{-1}}$) with a general anticyclonic circulation roughly following the local bathymetry. This weak flow is bordered to the east by relatively strong (up to $18\,\mathrm{cm\,s^{-1}}$) northwestward flow along the eastern flank of the Northern Kerguelen Plateau due to a northward bifurcation of cold Antarctic waters of eastern Enderby Basin origin carried by the powerful Fawn Trough Current. We have shown the utmost importance of the general circulation for the spatial distribution of primary productivity in that the sluggish circulation over the complex shallow topography of the Northern Kerguelen Plateau may precondition the recurrence of annual blooms, in contrast to neighboring strong advective regimes without blooming in deep water.

1. Introduction

Due to its great meridional extent (from 46°S to 64°S, based on the 3000 m isobath) and relatively shallow depths, the Kerguelen Plateau constitutes a major barrier to the eastward flowing Antarctic Circumpolar Current (ACC) in the Indian sector of the Southern Ocean. Park et al. (1991, 1993) showed, based on bottom-referenced geostrophic transports, that most (~100 Sv, $1\,\mathrm{Sv}=10^6\,\mathrm{m^3\,s^{-1}}$) of the ACC transport is deflected north of the Kerguelen Islands,

but with a substantial remainder (30–40 Sv) having to pass through the Antarctic Zone between the Kerguelen Islands and Antarctica. The Fawn Trough (sill depth: 2650 m at 56°S) splits the Kerguelen Plateau into two parts, the Northern and Southern Kerguelen Plateaus, and constitutes a favored zonal passage for the circumpolar flow crossing the plateau (Park et al., 1991; Park and Gambéroni, 1997; McCartney and Donohue, 2007; Roquet et al., 2008).

Due to the weak stratification and strong barotropicity of the Southern Ocean, bottom topography exerts a conspicuous steering effect on the circulation (e.g., Park et al., 2001). A zoomed stereoscopic bottom topography of

*Corresponding author. Tel.: +33 1 40 79 31 70; fax: +33 1 40 79 57 56.

E-mail address: yhpark@mnhn.fr (Y.-H. Park).

(A)

(B)

(C)
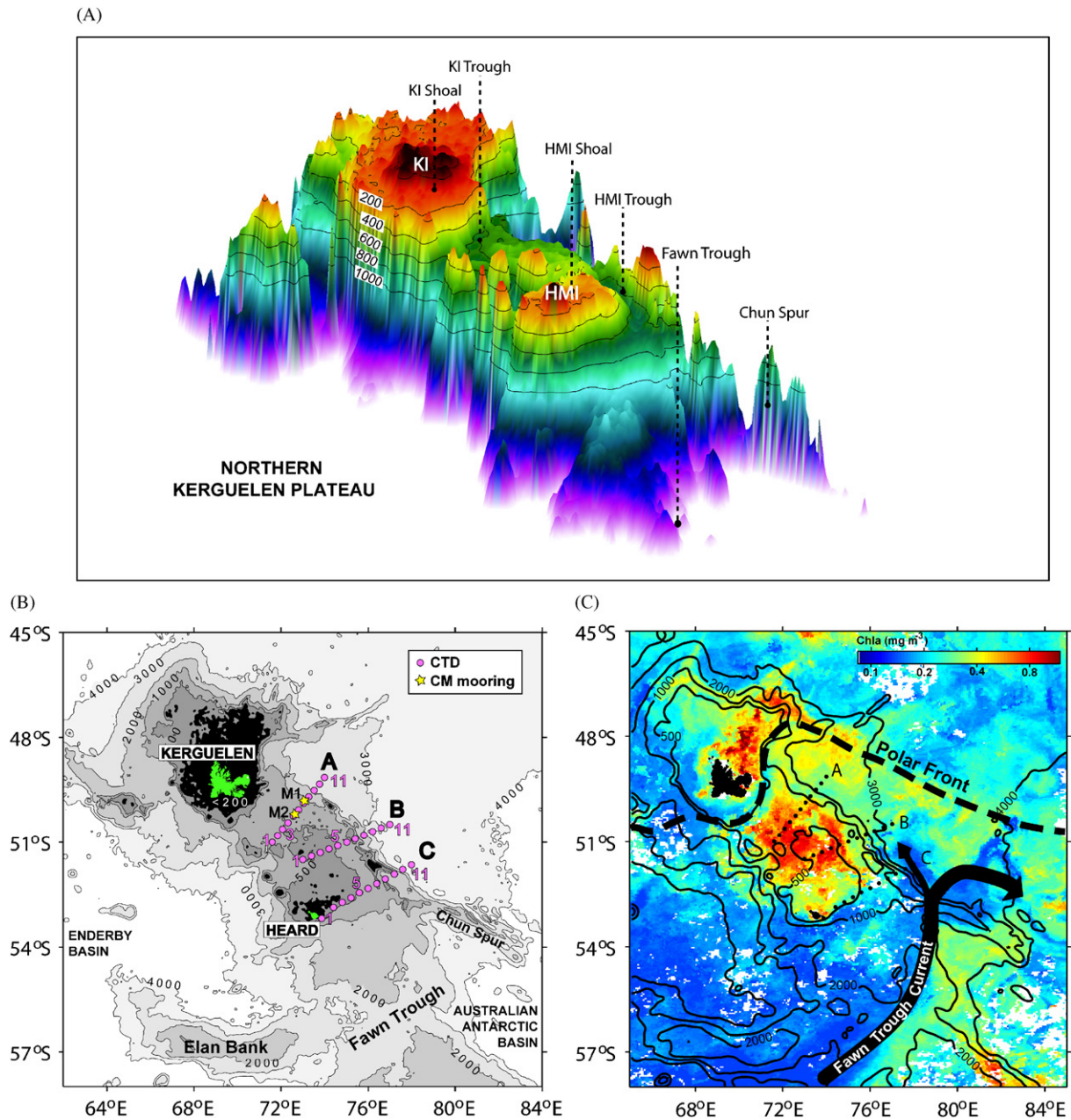
Fig. 1. (A) 3D view of the zoomed bathymetry shallower than 2000 m of the Northern Kerguelen Plateau constructed from the fine resolution ($2' \times 2'$) ETOPO2 bathymetric database. In the nomenclature, KI is for the Kerguelen Islands and HMI for the Heard/McDonald Islands. (B) Position of three CTD sections occupied during the January–February 2005 KEOPS cruise, superimposed on a 2D bottom topography. Isobaths are 4000, 3000, 2000, 1000, 500 m, and depths shallower than 200 m are shown in black. (C) Monthly mean chlorophyll concentration for January 2005 from MODIS data (courtesy of Mongin). The Polar Front from Park et al. (1998a) and the Fawn Trough Current from Roquet et al. (2008) are shown.

the Northern Kerguelen Plateau (Fig. 1A) reveals vividly the complexity of regional topography, which is otherwise difficult to imagine from a more conventional 2D representation (Fig. 1B). The Northern Kerguelen Plateau can be further split by a trough seen by the 600 m isobath at 50°30′S into two shoals around the Kerguelen and Heard/McDonald Islands. These are unnamed features, so we will call them tentatively the Kerguelen Islands Trough (KI Trough), Kerguelen Islands Shoal (KI Shoal), and Heard/McDonald Islands Shoal (HMI Shoal), respectively. The KI Shoal is very extensive and shallow (mostly less

than 200 m of water), while the HMI Shoal is deeper (<500 m) and smaller in size but accompanied by a number of seamounts close to the western flank of the plateau. The HMI Shoal is also separated from a chain of seamounts along the eastern edge of the plateau by a SE–NW oriented narrow trough, named here the HMI Trough, for convenience. We believe that this complex topography of the Northern Kerguelen Plateau may exert a significant influence on the local circulation, which needs to be taken into account when constructing a consistent large-scale circulation schematic.

In order to establish an oceanographic setting over the Northern Kerguelen Plateau for the natural iron fertilization experiment KEOPS (Blain et al., 2007), systematic hydrographic observations along three SW–NE oriented sections were made in January–February 2005, which cut the bloom center over the HMI Shoal across the eastern flank of the plateau into deep water (Fig. 1B). This productive area over the shallow platform is bounded on the north by the Polar Front developed along the KI Trough (Park and Gambéroni, 1997; Park et al., 1998b) and on the south by the Fawn Trough Current (McCartney and Donohue, 2007; Roquet et al., 2008). These can be easily depicted in satellite images as bands of low chlorophyll concentrations (Fig. 1C). The survey area thus appears as a sluggish environment surrounded by the strong current systems. However, a good knowledge of the hydrography and circulation of water masses seems to be necessary for better interpreting various biogeochemical and physical phenomena observed during our multidisciplinary cruise. The present paper is motivated to address such a requirement.

The eastern flank of the Southern Kerguelen Plateau has been relatively well exploited since the 1990s World Ocean Circulation Experiment (WOCE) period (Speer and Forbes, 1994; Donohue et al., 1999). From a detailed analysis of hydrographic observations along the WOCE section I8S cutting the eastern flank of the Southern Kerguelen Plateau at 58°S, McCartney and Donohue (2007) estimated an important northward transport (45 Sv) carrying Antarctic coastal waters along the eastern escarpment of the plateau. This section has recently been revisited by a collaborative Australian–Japanese expedition with a series of current meter moorings, consistently revealing the western boundary current (WBC) tightly attached to the escarpment (Aoki and Rintoul, 2005, personal communications). In contrast to this, no comparable systematic field experiments have been made over the Northern Kerguelen Plateau, aside from a recent use of penguins and elephant seals as autonomous oceanographic samplers (Charrassin et al., 2004; Roquet et al., 2008). Indeed, using temperature data from penguin-borne instrumentation, Charrassin et al. (2004) gave evidence of a subsurface cold water tongue flowing northwestward along the eastern flank of the Northern Kerguelen Plateau. This is consistent with Park and Gambéroni (1997) who showed a greater preponderance to the east of the Kerguelen Islands of colder and denser subsurface waters compared with those found west or south of the islands.

Although a rough circulation pattern of our study area emerges from previous studies (Park and Gambéroni, 1995; Park et al., 1998a; Charrassin et al., 2004), a circulation map sufficiently detailed to adequately interpret the KEOPS data is missing. This is because of the paucity of high-quality hydrographic data and of the presence of the widely developed, complex shallow topography of depths much shallower than 500 m, which makes the application of a deep reference level to the calculation of geostrophic currents difficult. In this paper we try to gather all available information to draw a consistent and comprehensive picture of the large-scale regional circulation.

2. Data

The principal new hydrographic data set used in this paper originates from the January–February 2005 KEOPS cruise carried out onboard the R/V Marion Dufresne. The hydrographic survey during the cruise consisted of a total of 121 Conductivity-Temperature-Depth (CTD) casts using a SeaBird 911-plus sounder, including many repeated casts. We focus on three sections (labelled A, B, and C) composed of 11 representative CTD profiles for each (Fig. 1B). These cut through the bloomed area of the HMI Shoal (Fig. 1C) and extend east across the rugged eastern flank of the Northern Kerguelen Plateau into deep water. The CTD casts were supplemented with 24 rosette water samples for analysis of salinity and dissolved oxygen. The CTD sensors were calibrated before and after the cruise. The post-cruise validated data for pressure, potential temperature, salinity, and dissolved oxygen are thought to be accurate within ± 3 dbar, $\pm 0.003\,^{\circ}$C, ± 0.005, and ± 0.005 ml l^{-1}, respectively.

In order to interpret the KEOPS observations within the general circulation context and to trace the upstream pathways of the observed water masses, we needed information of the circulation in a much larger area surrounding the Northern Kerguelen Plateau. For this end, we used, in addition to the KEOPS CTD data, all available historical hydrographic data for the area (40–60°S, 60–90°E) communicated by the SISMER/IFREMER (Systèmes d'Informations Scientifiques pour la Mer/Institut Français de Recherche pour l'Exploitation de la Mer), Brest. These include not only conventional hydrographic data but also autonomous ARGO float-derived CTD profiles quality-controlled by the CORIOLIS/IFREMER Project team. We also included recent Australian CTD data collected south and east of the Heard/McDonald Islands during the HIPPIES survey in December 2003 to February 2004 (Rosenberg, unpublished document, 2004) as well as hydrographic data derived from elephant seal-borne miniaturized CTDs deployed in 2004 over the entire Kerguelen Plateau (Roquet et al., 2008).

For describing a mid-depth current field of the area, we used velocity vectors at 900 m derived from Autonomous Lagrangian Circulation Explorer (ALACE) floats deployed since 1990 as part of the WOCE (Gille, 2003; Davis, 2005). Also used is a processed and corrected data set of near-surface velocities derived from Argos satellite-tracked drifting buoys (Pazan and Niiler, 2001; Niiler et al., 2003). For completeness, we referred to the altimetry-derived optimal solution of mean surface dynamic topography of Rio and Hernandez (2004) to validate different circulation patterns appearing from above data sets.

Although not fully exploited here, we have preliminary information of directly measured time-mean current profiles at two sites in section A (M1 and M2; see Fig. 1B for their positions), which were derived from two one-year-long moorings of up-looking acoustic Doppler current profilers (ADCP: 75 kHz RDI Long Ranger) recently recovered as part of the KEOPS experiment. These together with short-term (1–2 days) repeated measurements of current profiles using a lowered ADCP (LADCP: 300 kHz RDI) at two stations (A3, C11) during KEOPS were used for validating the bottom-referenced geostrophic velocities as well as our proposed circulation schematic.

3. Vertical structures of water masses and geostrophic currents during KEOPS

Vertical distributions of potential temperature, salinity, and oxygen content on the three CTD sections are shown in Fig. 2. Property–property correlation diagrams are shown in Fig. 3, although presenting separately those over the shallow platform (<600 m, station numbers 1–7 on each section) from the ones over the steep eastern escarpment (station numbers 8–11 on each section). This is because only limited water masses are found in the former region with often contrasting property distributions from the latter region due to different dynamics and circulations between the two regions. Useful information on these subtle differences, which could hint at the origins of water masses and their circulation patterns, may be discerned by a careful examination of the vertical property sections in combination with property–property correlations. Note that the supersaturation of oxygen at the surface seen in Fig. 3B is not due to data error but is a commonly observed feature in this sector of the Southern Ocean (e.g., Park et al., 1993).

3.1. Hydrographic characteristics over the plateau

We observe here a typical upper layer structure of the Antarctic Zone in the austral summer (e.g., Park et al., 1998a), which is best characterized below the surface mixed layer by a subsurface temperature minimum layer centered at around 200 m, the so-called Winter Water (WW). The temperature of the surface mixed layer (having a thickness of 70–100 m) ranges from 2.7 to 3.6 °C over the plateau, decreasing to the south (Fig. 2, panels A, B, C). However, the corresponding WW temperatures do not show such a monotonic decrease with latitude, but are highly variable according to sections and also to geographical positions even on the same section. For example, the greatest variability occurs on section C (C1–C7) where WW temperatures vary from a maximum of 2.2 °C at C4 to a minimum of 0.5 °C at C6 (see Fig. 3A). This is in great contrast to section A (A1–A7) where property–property correlations are most tightly established, with WW temperatures varying within a narrow range of

1.2–1.4 °C. Also remarkable is that the property–property correlations in section B (B1–B7) are heterogeneous and ill-defined. Moreover, WW temperatures there (1.6–2.0 °C) are significantly higher by about 0.5 °C than those in section A, despite the fact that the latter section is placed farther north by about 200 km, on average. This counter-intuitive feature in section B probably reflects enhanced turbulent mixing by tidal currents interacting with much shallower and rugged topography due to several surrounding seamounts in the west of the section (see Fig. 1A), possibly erasing the original WW characteristics by mechanical mixing with waters above and below. Similar mechanical mixing can be evoked for stations C1 and C4. On the other hand, stations C5 to C7 are unique in that they reveal the coldest WW (0.5–0.8 °C) as well as the Upper Circumpolar Deep Water (UCDW) that is unseen in other sections over the plateau. The latter water mass can be characterized by a subsurface temperature maximum and an oxygen minimum at about 500 m. Supporting visual evidence for these interpretations is given in Fig. 4 by selected vertical profiles of water properties. Station C6, where the coldest WW is observed, is located at the entrance to the northwestwardly elongated HMI Trough (of a maximum depth of 700 m) that is separated from the rugged eastern escarpment by a chain of shallow seamounts (~150–400 m) (see Fig. 1A). Considering this geomorphology and the observed water characteristics, this HMI Trough appears as a preferential northward pathway for waters originating from the south and flowing onto the plateau.

3.2. Hydrographic characteristics over the eastern escarpment

In contrast to the one over the shallow platform, the coldest (−0.4 °C) and most oxygenated (7.6 ml l^{-1}) WW over the steep eastern escarpment is found in section B (B9), not in the southernmost section C, where the local WW temperature minimum at C11 (0.1 °C) is warmer by about 0.5 °C than at B9 (see Fig. 3C). Another noticeable feature is that the WW over the escarpment is significantly denser ($\sigma_0 \sim 27.28$) than that over the platform ($\sigma_0 \sim 27.22$). Roquet et al. (2008) showed clearly that the coldest WW varieties of temperatures below zero are only found within the Fawn Trough Current originating from the eastern Enderby Basin south of 58°S. This suggests two important facts: (1) a branch of the Fawn Trough Current extends northward along the eastern flank of the Northern Kerguelen Plateau, transporting cold Antarctic waters of eastern Enderby Basin origin and travelling northward by more than 7° in latitude; (2) the core of this northward cold branch did not cut section C, at least during the KEOPS cruise, but should have passed somewhat east of C11. Due to the northward advection of cold Antarctic waters along the eastern flank of the plateau, a remarkable east-west contrast in WW temperature occurs between the shallow platform and the steep eastern escarpment. For example, at
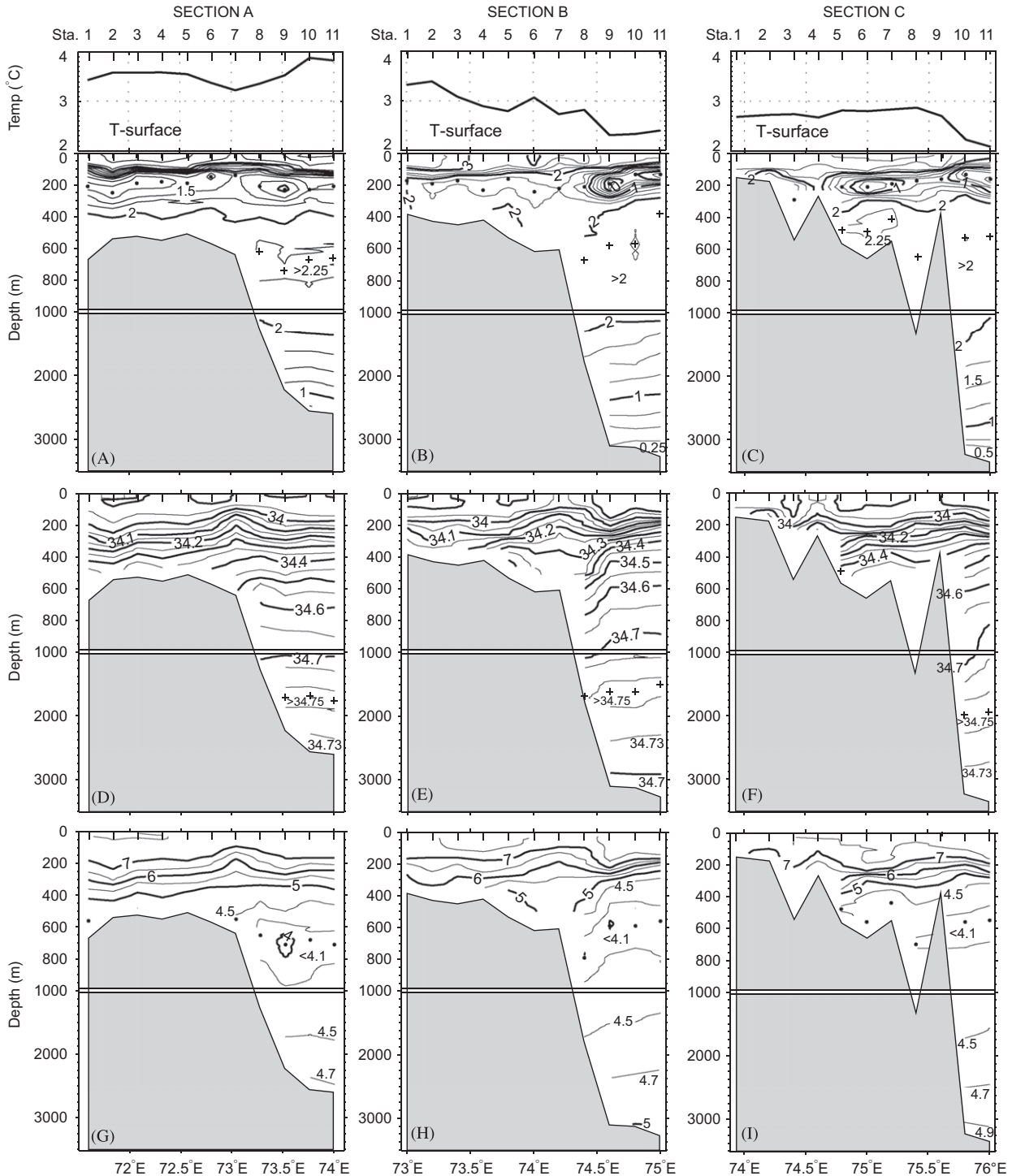
Fig. 2. Vertical distributions of potential temperature (A, B, C), salinity (D, E, F), and dissolved oxygen (G, H, I) on sections A, B, and C. Positions of maxima (minima) water properties are indicated by plus signs (dots). Surface temperatures along each section are shown in top panels. Note that the vertical scale of sections changes across the 1000 m depth.

the latitude of 51°S, the WW temperature over the eastern escarpment (e.g., B9) is up to 2 °C colder than that over the platform (e.g., A1). Such a northward advection of cold waters has previously been noticed as a subsurface cold-water tongue detected as far north as the latitude of the Kerguelen Islands (Park and Gambéroni, 1997; Charrassin et al., 2004).

Below the WW, we identify three water masses, namely: the UCDW associated with a temperature maximum and an oxygen minimum, as previously mentioned; the Lower Circumpolar Deep Water (LCDW) characterized by a deep salinity maximum; and the Antarctic Bottom Water (AABW) with decreasing temperature and salinity but sharply increasing oxygen content towards the bottom
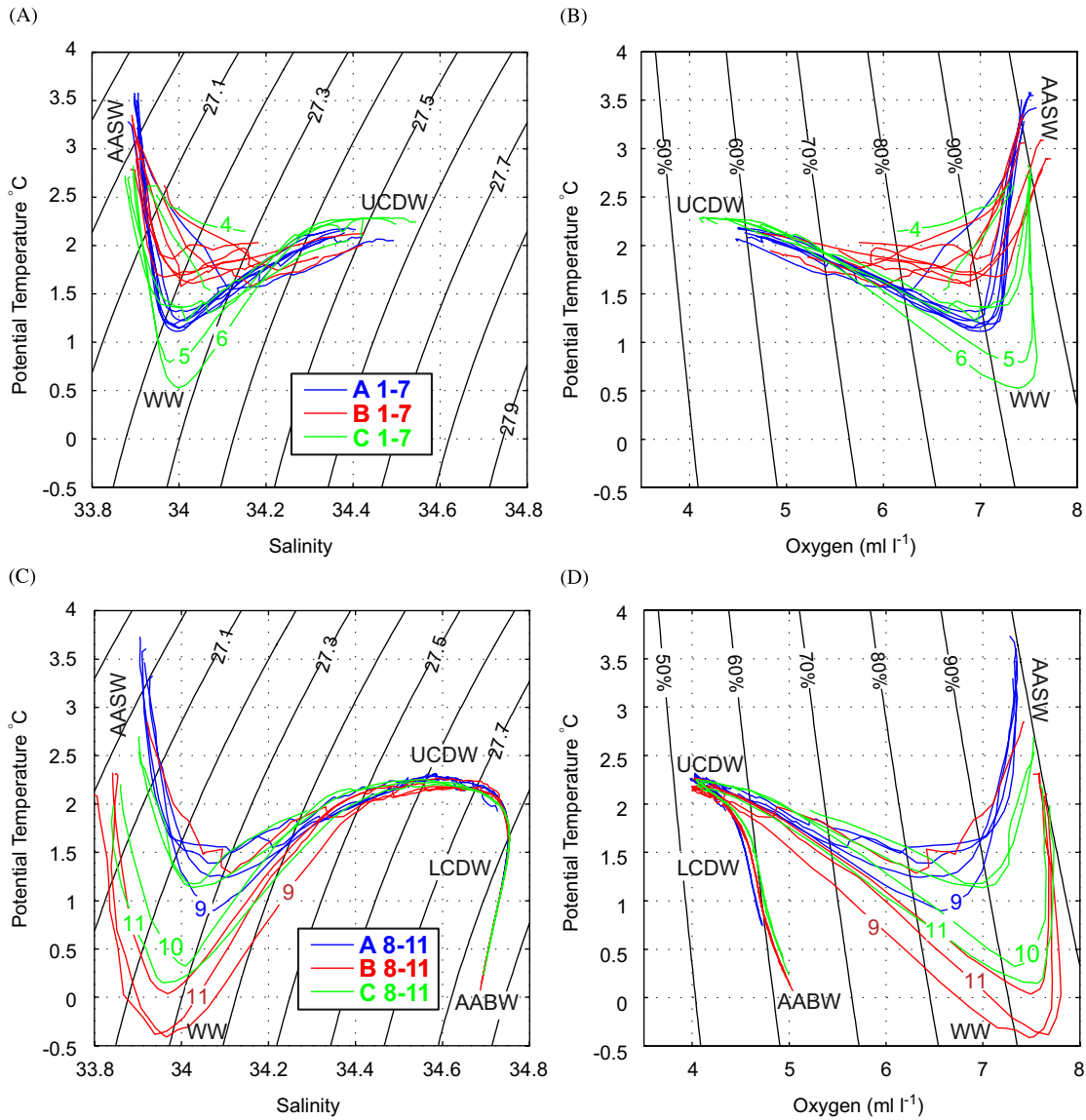
Fig. 3. Temperature–salinity and temperature–oxygen diagrams for stations over the shallow plateau (top) and those over the eastern escarpment (bottom). Major water masses identified are indicated: the Antarctic Surface Water (AASW), Winter Water (WW), Upper Circumpolar Deep Water (UCDW), Lower Circumpolar Deep Water (LCDW), and Antarctic Bottom Water (AABW).

(e.g., Park et al., 1993, 2001). In our area, these water masses were found roughly in the following depth intervals: 400 m < UCDW < 1400 m; 1400 m < LCDW < 2600 m; AABW > 2600 m.

Closer examination of Figs. 2 and 3 indicates that the deep and bottom waters in section B are significantly colder, less saline and more oxygenated than those on section C. This feature can be seen more clearly in the property profiles of the three deepest stations of each section (Fig. 5). Bottom property values at those stations are as follows: 0.24 °C, 34.695, 5.00 ml l^{-1} at 3300 m at C11; 0.07 °C, 34.685, 5.04 ml l^{-1} at 3220 m at B11; 0.75 °C, 34.717, 4.72 ml l^{-1} at 2530 m at A11. These observations indicate that the coldest, freshest and most oxygenated near-bottom water, i.e. the water of southernmost origin should have passed somewhere east of C11 before arriving

at B11. This feature is consistent with the afore-mentioned pathway of the northward branch of the Fawn Trough Current. We remark also that the oxygen profile at B11 shows a net change in its vertical gradient at around 2500 m, which is very close to the sill depth of the Fawn Trough (2650 m). This suggests that the water below 2600 m in section B should be a mixture with the AABW coming from the Antarctic coast along the eastern escarpment of the Southern Kerguelen Plateau south of the Fawn Trough (McCartney and Donohue, 2007). At C11, we observe a similar change in water characteristics below 3000 m, i.e. a depth 500 m deeper than at B11, indicating a more limited influence of the AABW at C11 compared to B11. Moreover, station B11 also reveals a sharp change in the LCDW properties below 1400 m, showing significantly colder, less saline, and more
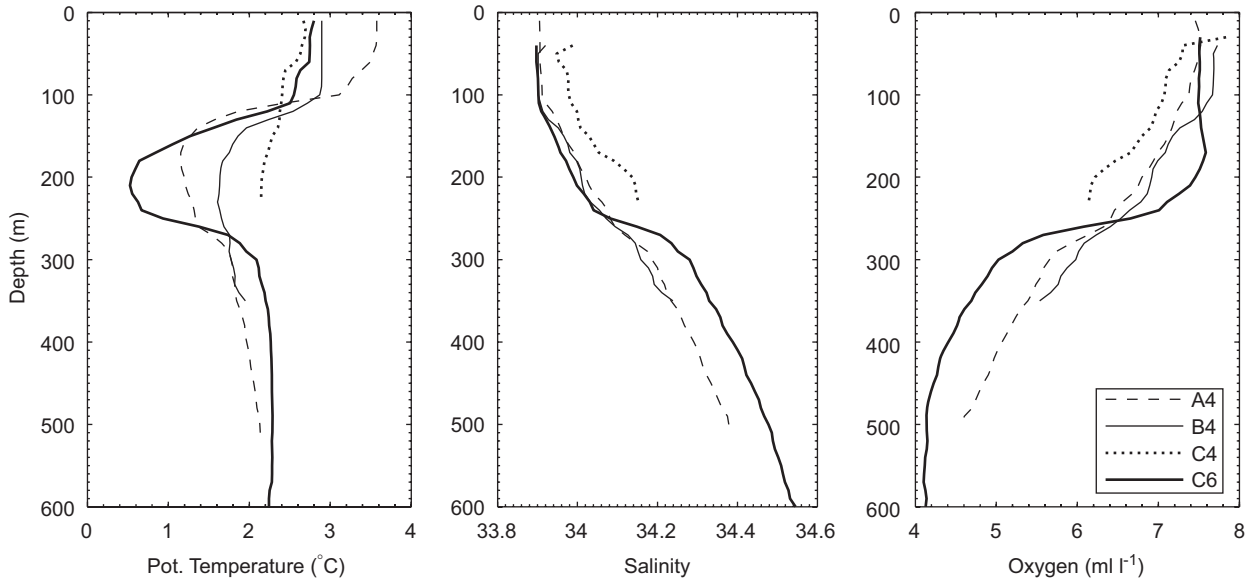
Fig. 4. Vertical profiles of temperature, salinity, and oxygen content for four selected stations over the shallow plateau.
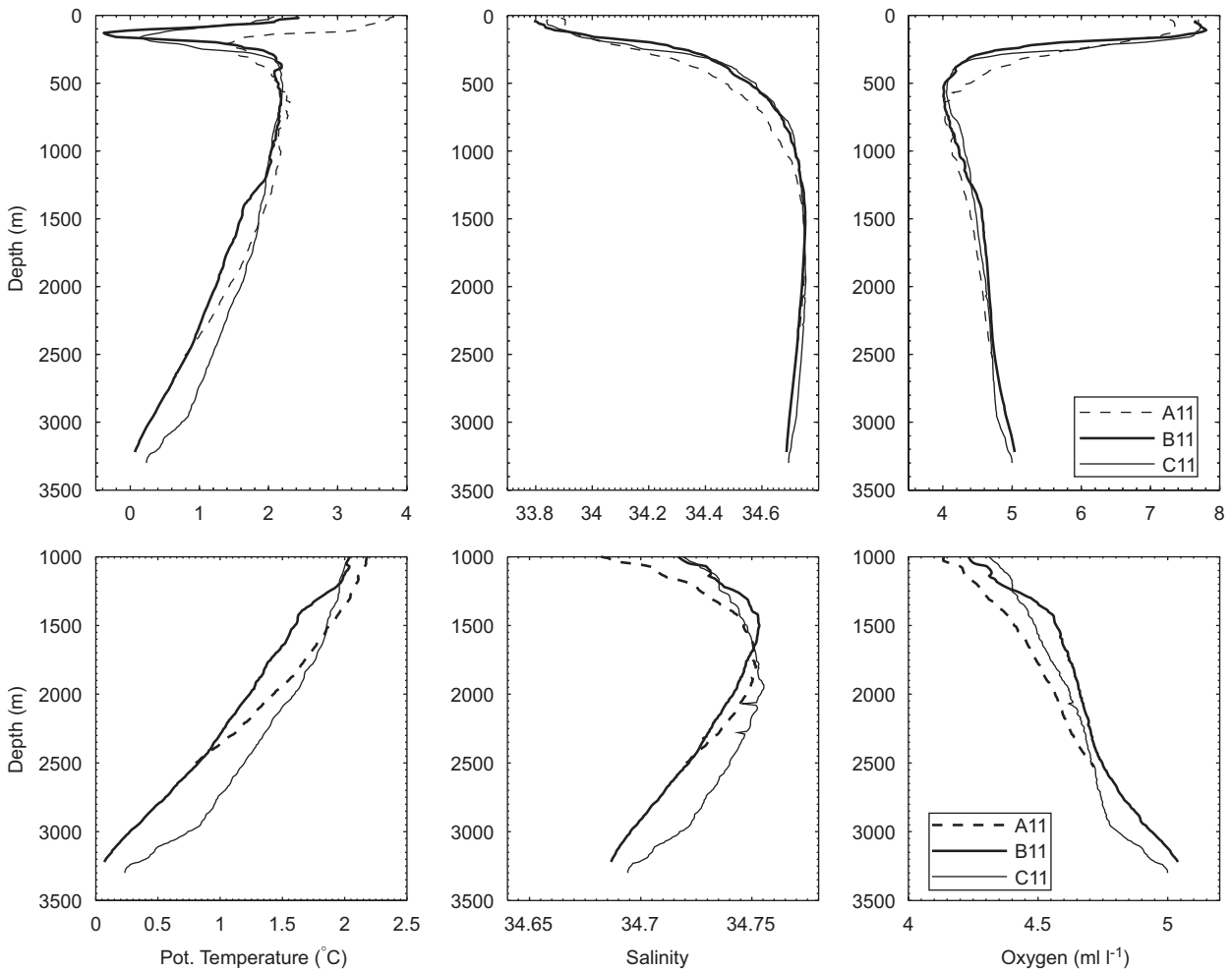
Fig. 5. (Top) Vertical profiles of temperature, salinity, and oxygen content for the easternmost stations A11, B11, and C11. (Bottom) Same as the top panels, but for zoomed profiles below 1000 m.

oxygenated profiles compared to the two other stations. This further strengthens our conjecture that B11 was placed precisely within the northward branch of the Fawn Trough Current. This can be explained by the fact that the latter current originates from far southern latitudes (Roquet et al., 2008) and that the LCDW property isolines in the Antarctic Zone shoal gradually toward Antarctica (e.g., Park et al., 2001). The latter fact also explains why property profiles at B11 appear shifted upward by about 500 m compared to those at C11 (see Fig. 5, bottom panels).

3.3. Geostrophic currents

We calculated geostrophic currents perpendicular to our three CTD sections relative to the deepest common depths between adjacent station pairs (Fig. 6). By this method, we obtain only the baroclinic shear relative to the bottom, which should underestimate (overestimate) the absolute geostrophic flow if the non-zero bottom flow has the same (opposite) sign as the shear. Based on the analysis of the one-year long current meter mooring data at M1 and M2 together with repeated LADCP measurements at A3 and C11 during KEOPS (see Appendix A), we are not certain that our bottom-referenced geostrophic calculation may be valid for weak velocities less than $3 \, \mathrm{cm \, s^{-1}}$. We did not try to constrain the geostrophic velocity to fit with the direct velocity measurements from the ship (using either the vessel-mounted ADCP or the CTD rosette-mounted LADCP) because instantaneous currents are dominated by tidal currents of velocities of order $20 \, \mathrm{cm \, s^{-1}}$ over the shallow platform (see Appendix A). The removal of these would require a highly accurate tide model with a velocity error of order $1 \, \mathrm{cm \, s^{-1}}$. In addition, there are also baroclinic (or internal) tidal currents of order $10 \, \mathrm{cm \, s^{-1}}$ (Park et al., 2008), a realistic modelisation of which also seems to be premature.

Calculated geostrophic currents over the shallow platform show a dominant northward component, except for the station pair A1–A2 where there appears a significant southward flow ($< 6 \, \mathrm{cm \, s^{-1}}$). Current speeds in section B are insignificantly weak (< 2–$3 \, \mathrm{cm \, s^{-1}}$). There is also an insignificant eddy-like feature between stations C1 and C5, probably due to shallow bathymetry close to the Heard/McDonald Islands. The strongest currents of the order of $8 \, \mathrm{cm \, s^{-1}}$ are found at the surface of section A (station pairs A2–A3 and A6–A7) only, while the aforementioned entrance to the HMI Trough in section C (station pair C5–C6) is associated with modest ($< 5 \, \mathrm{cm \, s^{-1}}$) northward flow.

Geostrophic currents over the eastern escarpment in sections B and C are all northward and much stronger by a factor of three to five than those over the shallow plateau. The strongest northward currents ($< 18 \, \mathrm{cm \, s^{-1}}$) are found in section B, tightly concentrated over the steep escarpment (station pair B8–B9), consistent with the aforementioned observations of the coldest ($-0.4 \, ^\circ\mathrm{C}$) and most oxygenated ($7.6 \, \mathrm{ml \, l^{-1}}$) WW there. The strongest currents in section C ($< 12 \, \mathrm{cm \, s^{-1}}$) are significantly weaker than those in section B and are found over the base of the escarpment (station pair C10–C11), which is also consistent with the second coldest WW observed at C11. Repeated LADCP measurements at C11 during KEOPS, although limited in time, also show consistent deep-reaching northward flow with a velocity stronger than $12 \, \mathrm{cm \, s^{-1}}$ at the surface and a depth-mean velocity of $8 \, \mathrm{cm \, s^{-1}}$. It is very likely that we are seeing there a part of the northward branch of the Fawn Trough Current whose core must have been located a little east of C11, as we have postulated using hydrographic features. Therefore, we may confirm that the strong northward flow at B8–B9 is the continuation of the northward branch of the Fawn Trough Current. Finally, farther north in section A, geostrophic currents over the escarpment are modest and mostly southward ($< 6 \, \mathrm{cm \, s^{-1}}$
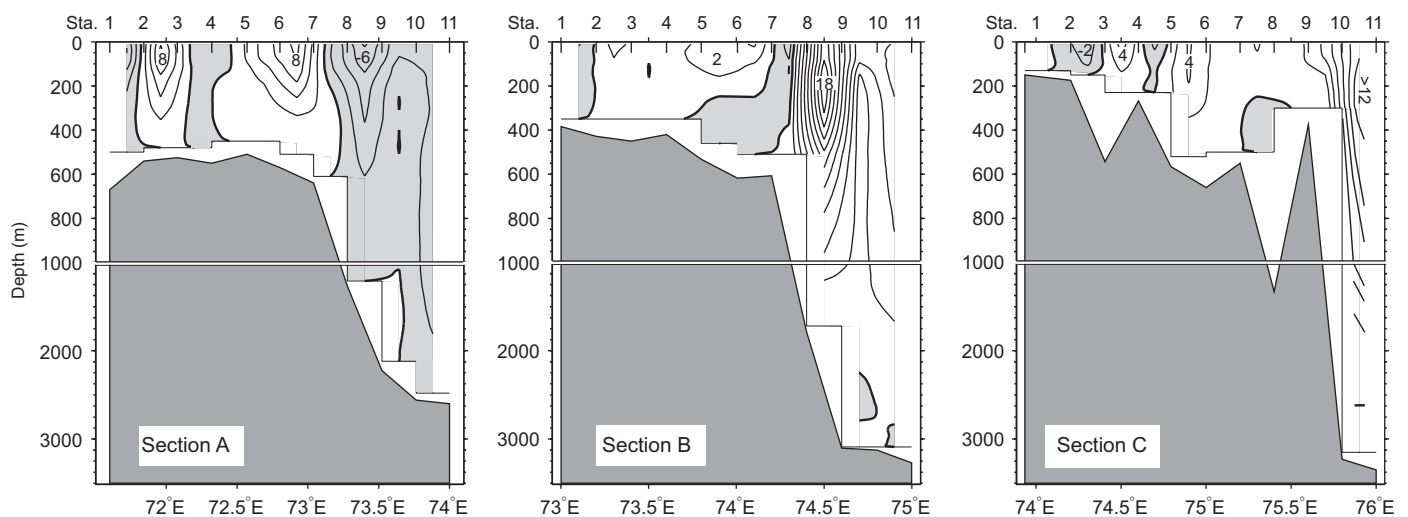
Fig. 6. Geostrophic speeds ($\mathrm{cm \, s^{-1}}$) relative to the deepest common sample depths for station pairs on the three KEOPS sections. Isotachs are every $2 \, \mathrm{cm \, s^{-1}}$. Shading indicates a southward flow. Note that the vertical scale of sections changes across the 1000 m depth.

at A8–A9, $<3\,\mathrm{cm\,s^{-1}}$ at A10–A11), although they are interrupted by a faint near-bottom northward flow at A9–A10. Considering the existence of the coldest WW ($0.9\,^{\circ}\mathrm{C}$) of the section at A9 (see Figs. 2 and 3), we suggest that the northward branch of the Fawn Trough Current, although much weakened, should have extended as far north as the latitude of the Kerguelen Islands, in agreement with previous work (Park and Gambéroni, 1997, Charrassin et al., 2004). The southward flow at A8–A9 thus appears to be contradictory to the presence of the coldest WW, suggesting that the direction of this modest flow might be wrong due to the inability of our method to detect the bottom intensified northward flow over the eastern escarpment. It also could be caused by some transient eddy activity. Unfortunately, our data set does not permit to be conclusive on this issue.

4. Circulation pattern and current field from historical data

4.1. Upper layer circulation pattern from hydrographic data

The general circulation of a region can be documented by mapping dynamic heights at a chosen level in reference to a deep reference level, assuming a zero or very weak flow at the latter level. In our case of the Kerguelen region, the shallow bottom topography of the Northern Kerguelen Plateau does not permit choosing a deep reference level commonly applicable to the entire domain. Despite this difficulty, we tried to map the near-surface (20 m) dynamic heights of the region relative to 500 m, in comparison with a map of potential density at 200 m (Fig. 7). Of course, it is not our intention to obtain an absolute geostrophic current field, especially in strong current regimes of deep surroundings where mid-depth currents are quite strong, as we will

see in the next subsection. We may expect, however, to gain some meaningful insight of the circulation pattern of relative baroclinic currents when both dynamic height and density maps show a similar spatial pattern. This is because a geostrophic flow can be considered, to a first approximation, as an isopycnal flow. Fig. 7 shows that such is in fact our case, permitting us to use either map to interpret the upper layer circulation pattern over the plateau in comparison with neighboring flows. However, we acknowledge that this method may fail in some areas where the bottom intensified barotropic flow is a significant contributor to absolute flow so that even the signs of flow can be wrong there. We will defer a critical comparison in reference to an altimetry-derived optimal inverse solution until Section 4.4.

In Fig. 7 we recognize without ambiguity two principal current systems rounding the Northern Kerguelen Plateau: the ACC and the Fawn Trough Current. The ACC north of the Kerguelen Islands (north of 47°S) hugs the northern escarpment, shifting gradually southward, while the Fawn Trough Current found initially south of the Elan Bank (south of 58°S) bends sharply to the north from 72°E to pass through the Fawn Trough. Therefore, the two currents initially flowing separately by a distance up to 11° in latitude in the west of the Kerguelen Plateau join each other just east of the plateau close to the outlet of the Fawn Trough Current in the Australian–Antarctic Basin (52°S, 82°E).

The flow over the Northern Kerguelen Plateau is sandwiched by those dominant currents and appears as a secondary circulation directed mostly to the northwest roughly in parallel with local bathymetry. This is related to the fact that the broad, featureless upstream flow imping-ing on the western flank of the plateau between the
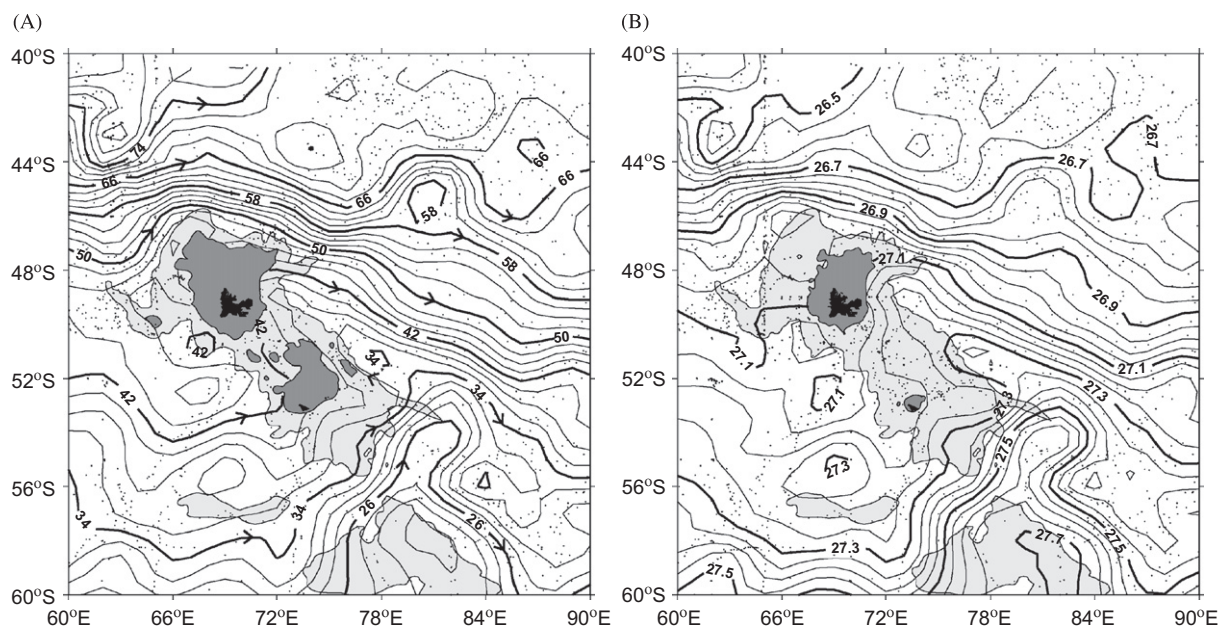
Fig. 7. (A) Dynamic heights (dyn cm) at 20 m relative to 500 m. Areas shallower than 2000 m (500 m) are lightly (darkly) shaded. (B) Potential density anomalies ($\mathrm{kg\,m^{-3}}$) at 200 m. Areas shallower than 2000 m (200 m) are lightly (darkly) shaded.

Kerguelen Islands and the Elan Bank do not cross directly over the plateau but bend sharply northward on approaching the western escarpment. Also, the streamlines running along the eastern flank of the plateau partly originate from the Fawn Trough Current, in agreement with the already-mentioned northwestward branch of the current evidenced from the KEOPS hydrographic data. All streamlines over the plateau converge in the east of the Kerguelen Islands before undergoing a complete retroflection to the southeast to merge into the southeastward flowing Polar Front. By geostrophy, this results in the development of a narrow band of dense water (or the so-called cold tongue) with somewhat depressed dynamic heights appearing along the eastern escarpment.

Finally, we note strong southeastward flow along the eastern flank of the Southern Kerguelen Plateau, which appears at odds with the northwestward-flowing deep WBC evidenced by McCartney and Donohue (2007), suggesting that our shallow reference level may not be adequate there. We will come back to this point later in Section 4.4.

4.2. Current field at 900 m from mid-depth floats

Davis (2005) presents maps of time-mean circulation at 900 m of the Indian and South Pacific Oceans measured by ALACE floats. However, only large-scale circulation patterns of spatial scales much greater than 300 km can be detected from these current fields constructed by spatial averaging using a decorrelation length scale of 300 km (Davis, 2005). Although useful for larger-scale oceanography, those maps are of only limited use for our Kerguelen region where interesting circulation features are of much smaller scales. Therefore, we examined instead original raw velocities (Gille, 2003; Davis, 2005). To isolate any subtle signatures of the secondary circulation around the Northern Kerguelen Plateau from noisy raw velocity vectors, the latter were ensemble averaged on a grid of 0.5° latitude by 1° longitude.

The resultant float-derived current field at 900 m is given in Fig. 8A, with several schematic streamlines guided by float trajectories being superimposed to aid interpretation. To be clear, we present in Fig. 8B four individual trajectories of ALACE with three additional ARGO floats drifting at different depths between 750 m and 2000 m. North of the Kerguelen Islands we see the powerful ACC with a width of 2–3° in latitude and a representative velocity of the order of 20–30 cm s^{-1}. Farther south, we see also the Fawn Trough Current of the order 10–20 cm s^{-1}, increasing to the east. It bends sharply to the north after its initial travel along the southern flank of the Elan Bank (57–58°S) to flow along the northern flank of the Fawn Trough close to the 2000-m isobath. It crosses the Chun Spur to penetrate into the Australian–Antarctic Basin as far north as 51°S, 82°E where it makes a cyclonic turn to flow southeastward. Another cyclonic feature (centered at 55°S, 81°E) is noticed just downstream from the Fawn
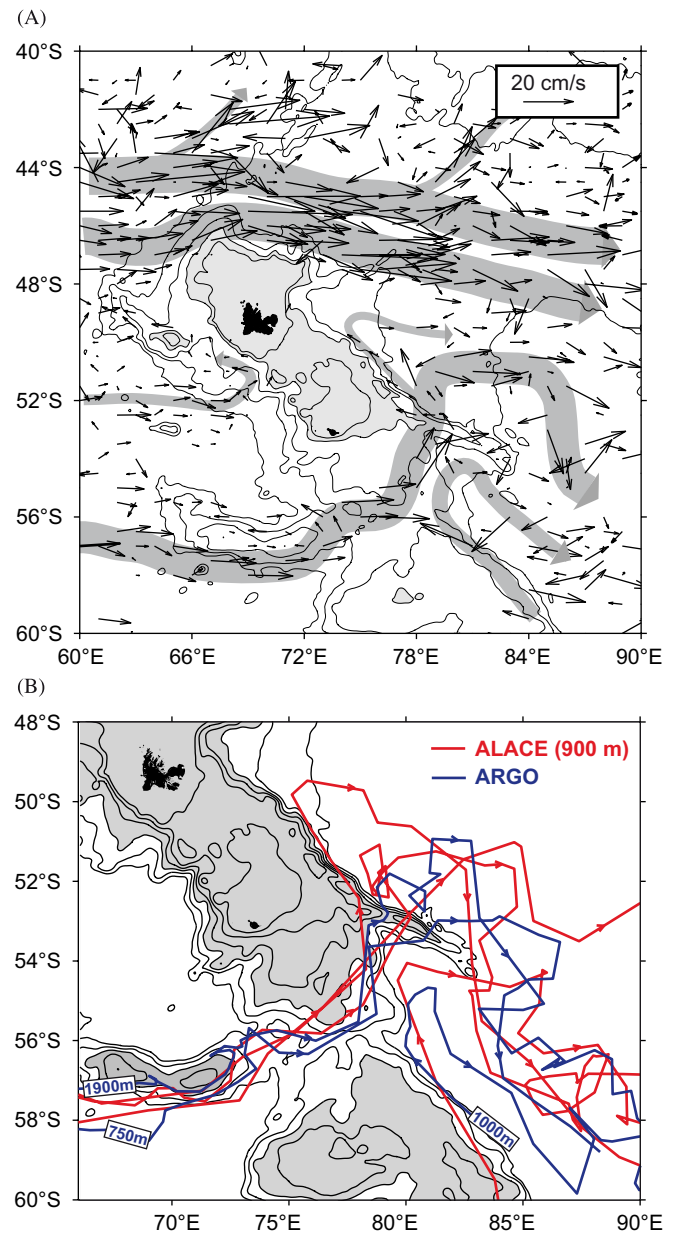
Fig. 8. (A) ALACE float-derived velocities at 900 m. The original velocity vectors (courtesy of Gille) were ensemble averaged on a 1° longitude by 0.5° latitude grid before mapping. Schematic stream lines are superimposed as guides. Areas shallower than 1000 m are shaded. (B) Trajectory of several selected ALACE (red) and ARGO (blue) floats which drifted either through the Fawn Trough or along the eastern escarpment of the Southern Kerguelen Plateau. Areas shallower than 2000 m are shaded.

Trough sill, which seems to play the role of junction with the WBC coming from the south along the eastern flank of the Southern Kerguelen Plateau (McCartney and Donohue, 2007). An interesting feature is the existence of several weak vectors (~5 cm s^{-1}) branching from the Fawn Trough Current at its outlet and extending northwestward along the eastern flank of the Northern Kerguelen Plateau up to 50°S where they undergo an abrupt southeast retroflection. In fact, these latter vectors are from a single float (Fig. 8B),

so the permanence of the feature cannot be ascertained. However, we have already given clear evidence for the existence of quasi-barotropic northward flow in the order of $8\,cm\,s^{-1}$ at C11 (see Fig. A1B) that is a site in close proximity to the float trajectory.

Although it is not the main focus of the present study, the circulation in the area east of the Fawn Trough sill, covering the eastern flank of the Southern Kerguelen Plateau and the Chun Spur, appears to be quite different from the schematic transport streamlines suggested by McCartney and Donohue (2007). According to these authors, the Fawn Trough Current turns south (rather than north as shown in Figs. 7 and 8) on its exit from the sill to join the south retroflection of the WBC initially flowing northwestward along the eastern flank of the Southern Kerguelen Plateau. They argue that the com-bined stream describes a subsequent east to north to northwest turn back, rounding the Chun Spur from the south, to return to the western boundary to the north of the spur. In Fig. 8B we see no evidence of a south turn of the Fawn Trough Current; rather all five floats passing through the Fawn Trough describe a remarkably compact along-isobath northeast pathway to cut near perpendicu-larly different places of the Chun Spur. The northwest-ward-flowing WBC of the Southern Kerguelen Plateau and its southeast retroflection offshore is clear, as already remarked by McCartney and Donohue (2007). However, we observe no trajectories showing a northwest turn-back rounding the southern end of the Chun Spur; rather we remark general southeastward flow, albeit with tumultuous meandering, in the area east and southeast of the spur.

4.3. Near-surface current field from drifting buoys

The raw near-surface velocities derived from drifting buoys were ensemble-averaged on the same grid ($0.5°$ latitude by $1°$ longitude) as for ALACE floats-derived velocities. The resulting map (Fig. 9) can be considered as showing the total near-surface velocity, i.e. the sum of the ageostrophic Ekman drift velocity and geostrophic velo-city. Although these surface velocities are much stronger by a factor of 2–3 than mid-depth velocities (Fig. 8A), the general circulation pattern is quite similar in both layers, showing the two principal current systems, the ACC and the Fawn Trough Current. Another interesting feature is the clear appearance of the Polar Front running eastward along $51°S$ until the immediate south of the Kerguelen Islands and then hugging anticyclonically the southern and eastern edge of the KI Shoal. This is not evident from hydrography, except in the eastern flank of the shoal (see Fig. 7).

Apart from these relatively well-defined current systems, our drifter currents do not fit well with the geostrophic circulation over the shallow platform. Aside from the northwestward flow associated with a bathymetry-follow-ing anticyclonic circulation in the southeastern side of the HMI Shoal, which agrees rather well with the
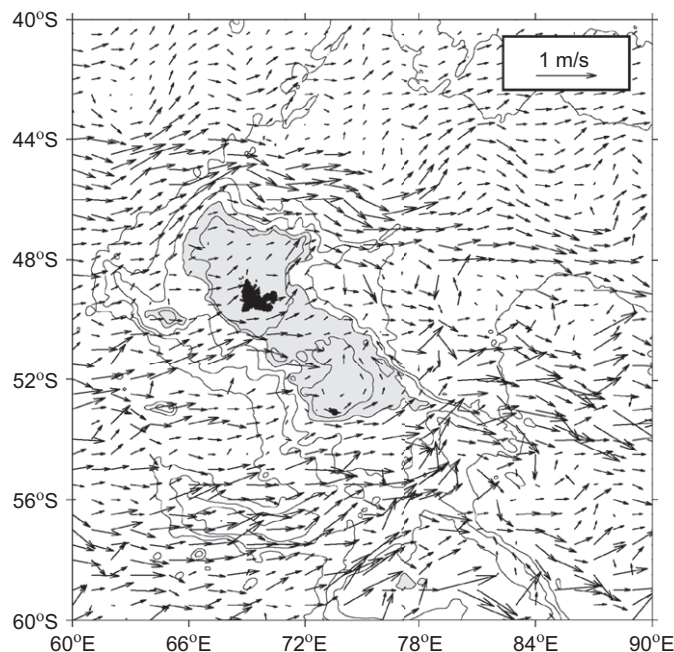
Fig. 9. Near-surface velocities derived from drifting buoys (courtesy of Niiler) averaged on a $1°$ longitude by $0.5°$ latitude grid. Areas shallower than 1000 m are shaded.

hydrographic solution (Fig. 7), there appears to be a general eastward flow in the drifter data. For example, all drifter vectors southeast of the KI Trough point to the east or northeast, in complete opposition to the northwestward flow seen from both hydrography (Fig. 7) and the one-year-long direct current measurements (Fig. A2). There is little evidence for the flow in the Fawn Trough turning northward and following the eastern flank of the Northern Kerguelen Plateau. In the western side of the HMI Shoal a great majority of drifter vectors are eastward, some of them even being abnormally strong.

Surface drifters include the Ekman drift that must have a northward component in this Southern Ocean area. Then, the dominance of eastward flow in the drifter data should imply general southeastward geostrophic flow over the plateau. This is exactly opposite to what is observed. Another abnormal feature appearing in the drifter data is that the current strength in the area south of the Kerguelen Islands, especially that of the Fawn Trough Current, appears to be unrealistically high compared to the ACC core north of the islands. A similar problem with the Southern Ocean drifter data has previously been remarked by Niiler et al. (2003) who showed that the surface geostrophic velocity derived from drifter data in the Southern Ocean is about 50% stronger than what is obtained from hydrographic data referenced to the ALACE float observations. These authors attribute this overestimation in the Southern Ocean to the high wind and concomitant large surface waves, which produce the Stokes drift causing increased slip of drifter drogues in the direction of the wind. For example, the Stokes drift for a $10\,m\,s^{-1}$ wind is in excess of $30\,cm\,s^{-1}$ in the direction of

the wind (Niiler et al., 2003). This information suggests that the drifter velocity field may not be so adequate for describing the surface circulation of the windy Southern Ocean, especially in a weak current area such as the shallow Northern Kerguelen Plateau. Therefore, we argue that this field must be considered as only indicative.

4.4. Altimetry-derived mean dynamic topography

As our final analysis of the surface circulation of the study area, we refer to the mean dynamic topography of Rio and Hernandez (2004). The first guess of this topography is obtained by subtracting the geoid model EIGEN-2 from the altimetric mean sea-surface height CLS01 and then merging with the Levitus climatology. This first guess is then improved by synthesizing all available information from in situ data (hydrological and drifter) combined with altimetric data using an inverse method (see Rio and Hernandez, 2004, for details). We present the resulting combined mean dynamic topography (CMDT Rio05, available at www.jason.oceanobs.com) of a spatial resolution of $0.5°$ latitude $\times 1°$ longitude in Fig. 10. As this solution optimally synthesizes useful information of various sources, it can be considered as the best currently available surface circulation of our study area. We discuss below the similarity and differences between this and different solutions already presented.

There is a good agreement among all solutions for the strong current systems such as the ACC north of the Kerguelen Islands and the Fawn Trough Current. In passing, however, we remark that the surface signature of

Fig. 10. Combined mean dynamic topography (CMDT Rio05) from Rio and Hernandez (2004). Streamlines are every 5 dyn cm. The isobaths 500 and 2000 m are shown. Arrows indicate the direction of the geostrophic flow.

the Fawn Trough Current south of the Elan Bank west of 75°E as seen from both the hydrographic and altimetric solutions (Figs. 7 and 10) is found about 1° south of the float-derived current (Fig. 8). In reference to the satellite images of chlorophyll concentrations (Fig. 1C; see also Mongin et al., 2008), the altimetric solution presents the most realistic position of the Polar Front, which in the hydrographic solution is only partly evident along the eastern flank of the KI Shoal. In the southern and eastern sides of the HMI Shoal, both the altimetric and hydrographic solutions show a bathymetry-following anticyclonic circulation. The general northwestward flow along the eastern side of the HMI Shoal and its southeast retroflection offshore are remarkably similar in these solutions. The direct connection of this northwestward flow with the Fawn Trough Current is not as apparent in these surface circulation maps; however, we have provided a number of supporting pieces of evidence for that connection from KEOPS hydrography (Section 3), LADCP measurements at C11 (Fig. A1), and float trajectories (Fig. 8). Therefore, we suggest that the northward bifurcation of the Fawn Trough Current and its northwestward extension along the eastern escarpment of the Northern Kerguelen Plateau should take place in the subsurface layer and deeper, i.e. it can be considered as a deep WBC.

The Southern Kerguelen Plateau counterpart of the deep WBC is best illustrated in float trajectories. Here, the sense of flow seems to be opposite within the water column, with insignificant southeastward flow in the surface layer as can be seen in the altimetric solution (Fig. 10) and strong northwestward flow at mid-depth as shown by float trajectories (Fig. 8). On the other hand, the surface dynamic heights relative to 500 m (Fig. 7) indicate rather strong southeastward flow close to the eastern flank, highly overestimating the flow velocity compared to the altimetric solution. This seems to be related to the fact that the employed dynamic method takes the velocity of the strong WBC at the reference level (500 m) as zero, by definition. The method thus fails there. Lastly, the circulation in the western side of the HMI Shoal is most ill defined. The sense of flow there is completely different among solutions: N to NW from hydrography (Fig. 7); E from drifters (Fig. 9); S to SE from altimetry (Fig. 10). This last solution is our favorite considering the southward velocity component observed at the westernmost stations in KEOPS sections A and B (Fig. 6). However, we refrain from drawing a formal conclusion, because this area where the bottom topography is very complex with a number of shallow seamounts, has not been well covered by KEOPS.

5. Conclusions

We have made a detailed analysis of the KEOPS CTD data in terms of the vertical structure of water masses and associated geostrophic currents. This analysis of in situ data within a limited area was extended to a more regional analysis of the general circulation using historical
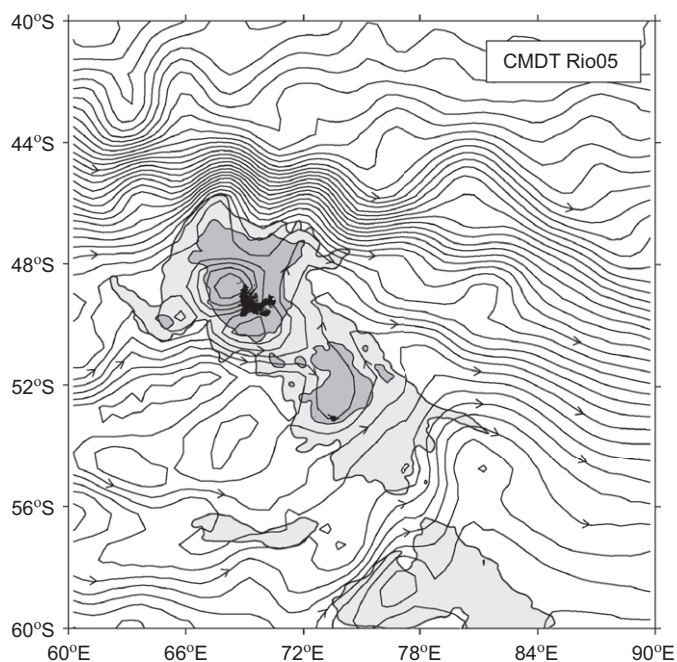
hydrographic data together with mid-depth and near-surface velocity information derived from ALACE floats, surface drifting buoys, and altimetry-derived optimal inverse solution. We found a number of common features appearing in both instantaneous and climatological fields. This suggests a quasi-permanent nature of most circulation features observed during KEOPS, which is likely related to the shallow topography of the plateau constantly steering the local circulation of water masses. This enables us to establish a synthetic picture of the upper layer circulation pattern over and around the Northern Kerguelen Plateau by combining all instantaneous and climatological information exploited in this study (Fig. 11). This schematic is sufficiently self-explanatory so that we do not feel it is necessary to reiterate a detailed description of each component of the general circulation already given in previous sections. We summarize rather that the KEOPS area appears as a ''cul de sac'' formed by surrounding strong current systems. The geostrophic circulation over the shallow platform is quite weak ($3-5 \, \text{cm s}^{-1}$) and anticyclonic, with the flow in the eastern side of the HMI Shoal consistently northwestward, a direction perpendicular or opposed to the dominant westerlies of the region. This feature appears to be somewhat surprising at a first glance; however, it is strongly supported by depth-averaged (over the first 500 m depth) time-mean currents directly measured by one-year-long current meter moorings at M1 ($6 \, \text{cm s}^{-1}$, 296°) and M2 ($4 \, \text{cm s}^{-1}$, 264°), as well as by repeated LADCP measurements at A3 ($3 \, \text{cm s}^{-1}$, 8°) and C11 ($11 \, \text{cm s}^{-1}$, 344°) (see Appendix A). Compared to this

relatively robust northwestward flow in the eastern side, the circulation in the western side of the HMI Shoal is much less well defined, although we propose that there is a tentatively weak topography—following southward flow. The verification of this is left to a future study. The most remarkable feature clearly identified by the present study is a much stronger (up to $18 \, \text{cm s}^{-1}$) northwestward branch of the Fawn Trough Current, which advects cold Antarctic waters of eastern Enderby Basin origin along the eastern flank of the Northern Kerguelen Plateau.

By comparing this schematic with the satellite image of chlorophyll in Fig. 1C, it is not difficult to ascertain that annual blooms develop only within sluggish areas in shallow water surrounded by strong currents, such as our KEOPS survey area over the HMI Shoal and the KI Shoal widely developed north of the Kerguelen Islands. Park et al. (2008) discuss this topic in details, in relation to elevated vertical mixing due to strong activity of internal tides observed at A3. The present study is complementary to that work, providing a consistent and comprehensive upper-layer circulation over and around the Northern Kerguelen Plateau and emphasizing the importance of the sluggishness of local circulation for preconditioning the recurrence of annual blooms.

Finally, we note that the region downstream from the Fawn Trough sill, which forms a semi-enclosed basin surrounded by the southeastern flank of the Northern Kerguelen Plateau to the west and the Chun Spur to the northeast, appears as a potentially important place of mixing where the waters of Antarctic coast origin carried
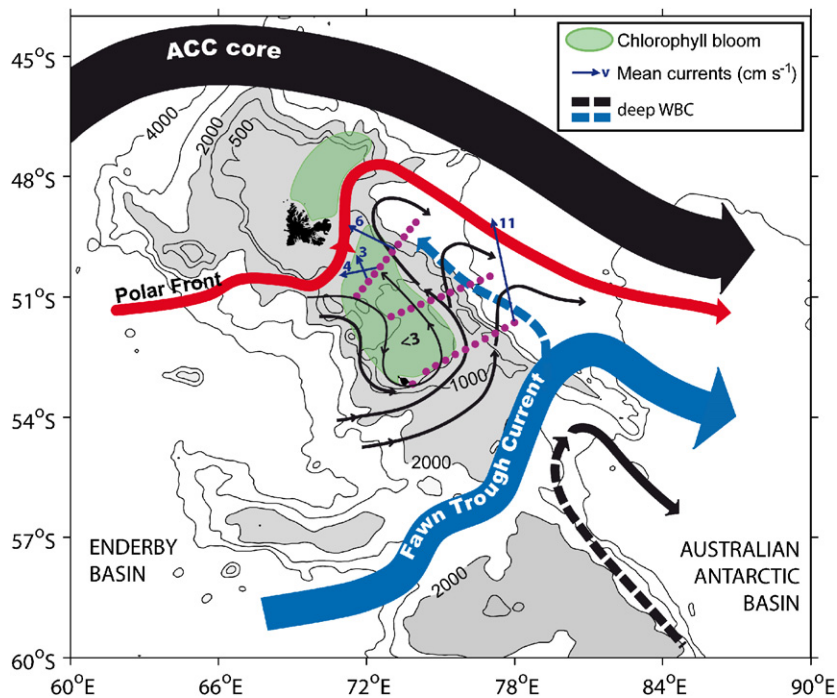
Fig. 11. Schematic of the geostrophic circulation over and around the Kerguelen Plateau based on the synthesis of our major findings. Thin arrows with Arabic numerals stand for directly measured time-mean current vectors averaged over the upper 500 m layer (see the text for details; see also Figs. A1 and A2). Subsurface western boundary currents are indicated by discontinuous bold lines. The apparent linkage between areas of annual chlorophyll bloom and those of a sluggish flow surrounded by strong currents is stressed.

north by the strong WBC along the eastern flank of the Southern Kerguelen Plateau meet the Enderby Basin waters carried by the Fawn Trough Current. We have shown that the latter current shifts to the north along the southeastern flank of the Northern Kerguelen Plateau before crossing the Chun Spur, consistent with the results from elephant seal data (Roquet et al., 2008). In the upper 2000 m, there does not appear any evidence of the northwest turn back of flow to the north of the Chun Spur as suggested by McCartney and Donohue (2007), although such a circulation pattern cannot be ruled out in deeper layers. To document better the local circulation and mixing of water masses, and to quantify the Fawn Trough Current transport and its variability, an extensive CTD survey in this mixing zone during 2009 with three lines of one year-long current meter moorings across the Fawn

Trough sill is being planned in the framework of the International Polar Year (Park, unpublished document, 2006).
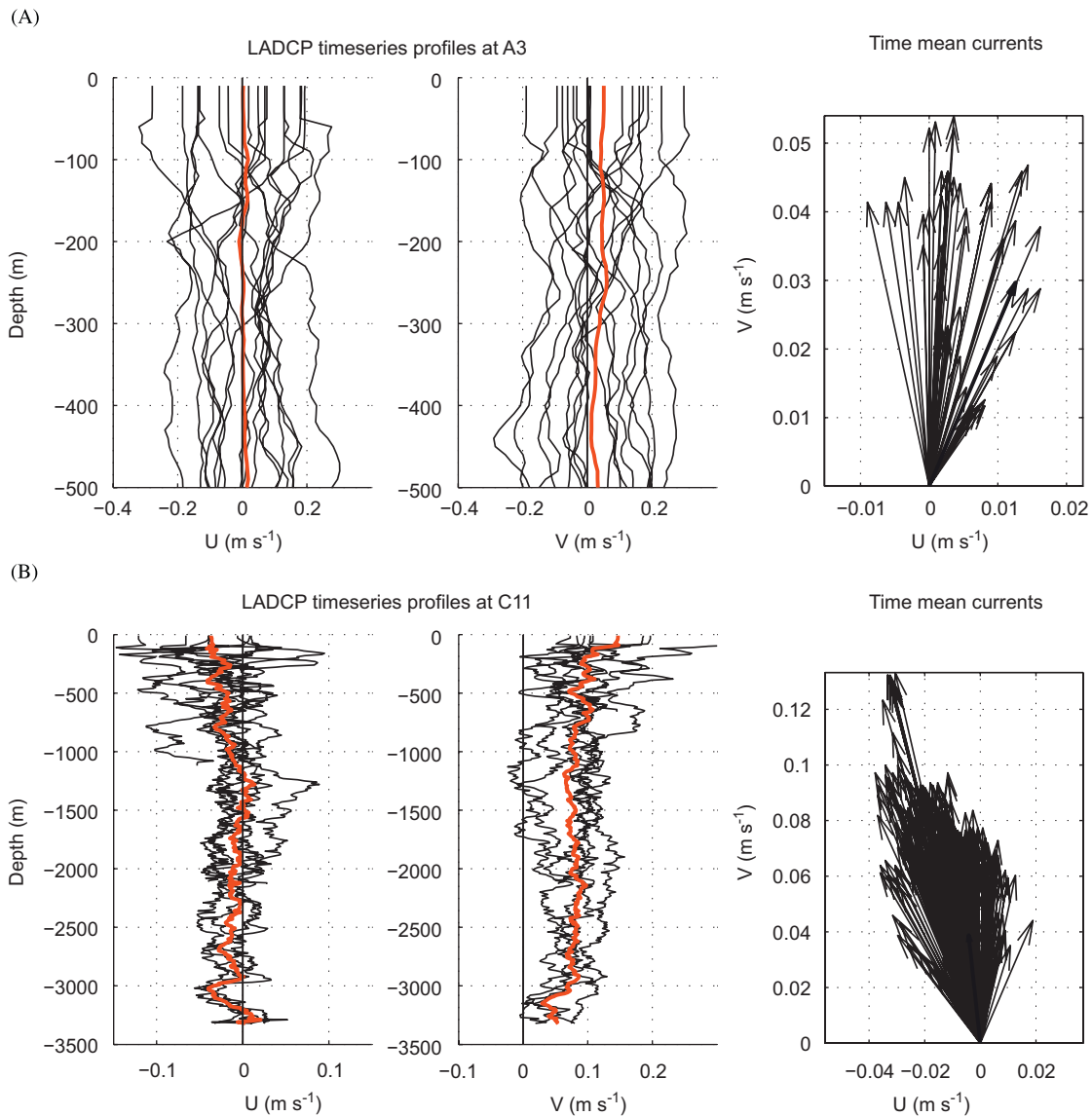
Fig. A1. Repeated LADCP measurements at (A) station A3 and (B) station C11 (see Fig. 1b for their positions). For both stations, the zonal (left) and meridional (middle) current profiles are shown in black together with the time-mean current profiles in red. In the right panels, time-mean current vectors are shown every 10 m in vertical. Note the different scales of time-mean currents used for A3 and C11.
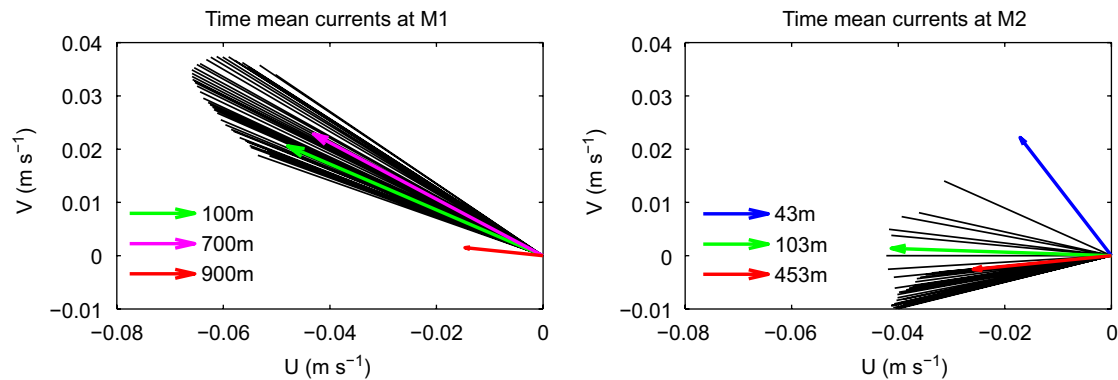
Fig. A2. One-year-mean current vectors at mooring sites M1 (left) and M2 (right). Both moorings contained an up-looking ADCP placed at the nominal depth of 500 m. For M1, two supplementary RCM current meters were placed at 700 and 900 m. ADCP velocity vectors are every 10 m beginning from 100 m for M1 and 43 m for M2. Velocity vectors at several selected depths are shown in color.

Appendix A. Validity of the bottom reference level in the KEOPS area

In order to estimate the degree to which our estimation of geostrophic currents is affected by the choice of the bottom level of no motion, we examine first the repeated measurements of LADCP profiles at A3 and C11 (Fig. A1). Over the shallow plateau (A3), tidal currents of an amplitude of 20 cm s^{-1} constitute a predominant component of total currents, and the time-mean currents over 36-h represent less than 20% ($<$5 cm s^{-1}) of the total currents, with a dominant direction to the north throughout the water column (Fig. A1A). In deep water at the base of the eastern escarpment (C11), tidal currents are much weaker by a factor of three than those over the shallow platform, but the average currents of a total of eight repeated profiles made at time intervals of 2- to 3-h are as strong as tidal currents ($<$10 cm s^{-1}) with a predominant NNW direction throughout the 3300 m water column (Fig. A1B). At this station, the southward velocity component was rarely recorded during the whole period of repeated LADCP measurements. However, we consider these results as only indicative because the time interval used for averaging is too short to yield statistically meaningful time-mean values.

For this latter end, we show in Fig. A2 the one-year mean current vectors in the water column at two mooring sites near A7 ($\sim$1000 m depth, M1 hereafter) and A5 ($\sim$500 m depth, M2 hereafter) (see Fig. 1B for their geographical positions). At both sites, current measurements were made by up-looking ADCPs moored at around the 500 m depth, with two supplementary RCM current meters at 700 and 900 m at M1. The ADCP-derived time-

mean currents are shown every 10 m from 100 to 560 m for M1 and from 43 to 453 m for M2. The one-year mean near-bottom currents are 1.6 cm s^{-1}, 276° at M1 and 2.9 cm s^{-1}, 264° at M2, both showing an anticlockwise veering by 30–60° compared to the upper layer. All this information, although not exhaustive, suggests that our bottom referenced geostrophic currents could be biased by up to 3 cm s^{-1} at some places over the shallow platform. Consequently, in a weak current area of velocities $<$3 cm s^{-1} our method may not work well and even the correct sense of flow cannot be guaranteed.

References

Blain, S., Quéguiner, B., Armand, L., Belviso, S., Bombled, B., Bopp, L., Bowie, A., Brunet, C., Brussard, C., Carlotti, F., Christaki, U., Corbière, A., Durand, I., Ebersbach, F., Fuda, J.-L., Garcia, N., Gerringa, L., Griffiths, B., Guigue, C., Guillerm, C., Jaquet, S., Jeandel, C., Laan, P., Lefèvre, D., Lomonaco, C., Malits, A., Mosseri, J., Obernosterer, I., Park, Y.-H., Picheral, M., Pondaven, P., Remeny, T., Sandroni, V., Sarthou, G., Savoye, N., Scouarnec, L., Souhaut, M., Thuiller, D., Timmernans, K., Trull, T., Uitz, J., van-Beek, P., Veldhuis, M., Vincent, D., Viollier, E., Vong, L., Vagner, T., 2007. Effect of natural iron fertilization on carbon sequestration in the Southern Ocean. Nature 446.

Charrassin, J.-B., Park, Y.-H., Le Maho, Y., Bost, C.-A., 2004. Fine resolution 3D temperature fields off Kerguelen from instrumented penguins. Deep-Sea Research I 51, 2091–2103.

Davis, R.E., 2005. Intermediate-depth circulation of the Indian and South Pacific Oceans measured by autonomous floats. Journal of Physical Oceanography 35, 683–707.

Donohue, K.A., Hufford, G.E., McCartney, M.S., 1999. Sources and transport of the deep western boundary current east of the Kerguelen Plateau. Geophysical Research Letters 26, 851–854.

Gille, S.T., 2003. Float observations of the Southern Ocean. Part I: estimating mean fields, bottom velocities, and topographic steering. Journal of Physical Oceanography 33, 1167–1181.

McCartney, M.S., Donohue, K.A., 2007. A deep cyclonic gyre in the Australian-Antarctic Basin. Progress in Oceanography 75, 675–750.

Mongin, M., Molina, E., Trull, T., 2008. Seasonality and scale of the Kerguelen plateau phytoplankton bloom: a remote sensing and modeling analysis if the influence of natural iron fertilization in the Southern Ocean. Deep-Sea Research II, this issue [doi:10.1016/j.dsr2.2007.12.039].

Niiler, P., Maximenko, N.A., McWilliams, J.C., 2003. Dynamically balanced absolute sea level of the global ocean derived from

near-surface velocity observations. Geophysical Research Letters 30 (22), 2164.

Park, Y.-H., Gambéroni, L., 1995. Large-scale circulation and its variability in the South Indian Ocean from TOPEX/POSEIDON altimetry. Journal of Geophysical Research 100, 24,911–24,929.

Park, Y.-H., Gambéroni, L., 1997. Cross frontal injections of Antarctic intermediate water and Antarctic bottom water in the Crozet Basin. Deep-Sea Research II 44, 963–986.

Park, Y.-H., Gambéroni, L., Charriaud, E., 1991. Frontal structure, transport and variability of the Antarctic Circumpolar Current in the South Indian Ocean sector, 40°–80°E. Marine Chemistry 35, 45–62.

Park, Y.-H., Gambéroni, L., Charriaud, E., 1993. Frontal structure, water masses, and circulation in the Crozet Basin. Journal of Geophysical Research 98, 12361–12385.

Park, Y.-H., Charriaud, E., Fieux, M., 1998a. Thermohaline structure of the Antarctic surface water/winter water in the Indian sector of the Southern Ocean. Journal of Marine Systems 17, 5–23.

Park, Y.-H., Charriaud, E., Ruiz Pino, D., Jeandel, C., 1998b. Seasonal and interannual variability of the mixed-layer properties and steric height at station KERFIX southwest of Kerguelen. Journal of Marine Systems 17, 233–247.

Park, Y.-H., Charriaud, E., Craneguy, P., Kartavtseff, A., 2001. Fronts, transport, and Weddell Gyre at 30°E between Africa and Antarctica. Journal of Geophysical Research 106, 2857–2879.

Park, Y.-H., Fuda, J.L., Durand, I., Naveira Garabato, A.C., 2008. Internal tides and vertical mixing over the Kerguelen Plateau. Deep-Sea Research II, this issue [doi:10.1016/j.dsr2.2007.12.027].

Pazan, S., Niiler, P., 2001. Recovery of near-surface velocity from undrogued drifters. Journal of Atmospheric and Oceanographic Technology 18, 476–489.

Speer, K.G., Forbes, A., 1994. A deep western boundary current in the South Indian Basin. Deep-Sea Research I 41, 1289–1303.

Rio, M.-H., Hernandez, F., 2004. A mean dynamic topography computed over the world ocean from altimetry, in-situ measurements and a geoid model. Journal of Geophysical Research 109, C12032.

Roquet, F., Park, Y.-H., Guinet, C., Bailleul, F., Charrassin, J.-B., 2008. Observations of the Fawn Trough Current over the Kerguelen Plateau from instrumented elephant seals. Journal of Marine Systems, accepted for publication.